

Identifying True Vessels Using Krisch Edge Segmentation

¹K.A.Nithya, ²Aruchamy Rajini

¹Research Scholar, Department of Computer Science, Hindustan college of Arts and Science, Coimbatore, India

²Associate professor, Department of Computer Science, Hindustan college of Arts and Science, Coimbatore, India

Abstract: Measurements of retinal blood vessel morphology have been shown to be related to the risk of cardiovascular diseases. The wrong identification of vessels may result in a large variation of these measurements, leading to a wrong clinical diagnosis. In this paper, address of the problem identifying true vessels as a post processing step to vascular structure segmentation. These model segmented vascular structure as a vessel segment graph and formulate the problem of identifying vessels as one of finding the optimal forest in the graph given a set of constraints.

Index Terms: Ophthalmology, optimal vessel forest, retinal image analysis, simultaneous vessel identification, vascular structure.

I. INTRODUCTION

A RETINAL image provides a snapshot of what is happening inside the human body. In particular, the state of the retinal vessels has been shown to reflect the cardiovascular condition of the body. Measurements to quantify retinal vascular structure and properties have shown to provide good diagnostic capabilities for the risk of cardiovascular diseases. For example, the central retinal artery equivalent (CRAE) and the central retinal vein equivalent (CRVE) are measurements of the diameters of the six largest arteries and veins in the retinal image, respectively. These measurements are found to have good correlation with hypertension, coronary heart disease, and stroke.[1-3] However, they require the accurate extraction of distinct vessels from a retinal image. This is a challenging problem due to ambiguities caused by vessel bifurcations and crossovers.



Fig. 1(a)

Fig. 1(a) shows an example retinal image where vessels I and II cross each other at two places (indicated by circles). These crossovers are often

mistaken as vessel bifurcations, leading to I and II being regarded as a single vessel.



Fig. 1(b)

Fig. 1(b) shows the correctly identified vessel structures for vessels I and II marked in blue and red, respectively. Note that the line segment at the second crossing (larger circle) is shared by vessels I and II. In order to disambiguate between vessels at bifurcations and crossovers, in need to figure out if linking a vessel segment to one vessel will lead to an adjacent vessel being wrongly identified.

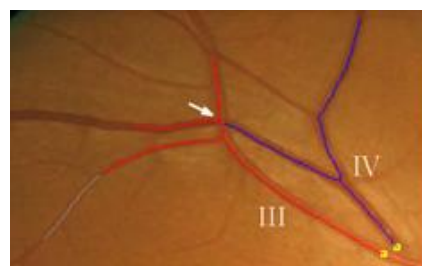


Fig. 2(a)

For example, in Fig. 2(a), if they identify vessel III first without any knowledge of vessel IV, the junction indicated by the white arrow may be mistaken as a bifurcation instead of a crossover. Consequently, vessels III and IV will be incorrectly identified, leading to a large difference in vessel measurements. However, if both vessels were constructed and considered at the same time, it becomes obvious that one of the branches of vessel III should be an extension of vessel IV, as shown in Fig. 2(b).

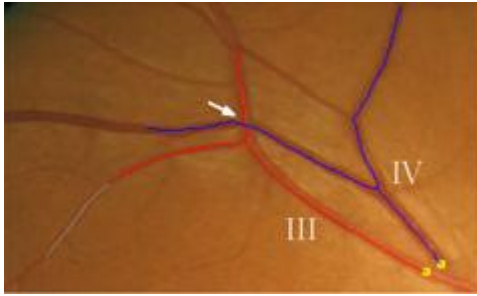


Fig.2(b)

By considering multiple vessels simultaneously, information from other vessels can be used to better decide on the linking of vessel segments. In this paper, describe a novel technique that utilizes the global information of the segmented vascular structure to correctly identify true vessels in a retinal image. These model the segmented vascular structure as a vessel segment graph and transform the problem of identifying true vessels to that of finding an optimal forest in the graph. An objective function to score forests is designed based on directional information.[3-4] In proposed solution employs candidate generation and expert knowledge to prune the search space.

II. LITERATURE SURVEY

Image processing is the perception of several algorithms that take an image as input and proceeds an image as output. Retinal vessel extraction involves segmentation of vascular structure and identification of distinct vessels by linking up segments in the vascular structure to give complete vessels. One branch of works, termed vessel tracking, performs vessel segmentation and identification at the same time [5]–[8]. Another branch of works treat vessel identification as a preprocessing step to segmentation [9]–[11]. The work in [9] required the user to resolve the connectivity of bifurcation and crossover points before vessels were individually identified. For [10], a graph formulation was used with Dijkstra's shortest path algorithm to identify the central vein. Similarly, Joshi *et al.* [11] used Dijkstra's algorithm to identify vessels one at-a-time. Al-Diri *et al.* [12] used expert rules to resolve vessel crossovers and locally linked up segments at these crossovers to give a vascular network. This work is

focused on vessel identification as a post processing step to segmentation. In this approach differs from existing works in that identify multiple vessels simultaneously and use global structural information to figure out if linking a vessel segment to one vessel will lead to an overlapping or adjacent vessel being wrongly identified.

III. VESSEL SEGMENTATION

A. Preprocessing

Color fundus images often show important lighting variations, poor contrast and noise. In order to reduce these imperfections and generate images more suitable for extracting the pixel features demanded in the classification step, a preprocessing comprising the following steps is applied:

1) *Vessel Central Light Reflex Removal*: Since retinal blood vessels have lower reflectance when compared to other retinal surfaces, they appear darker than the background. To remove this brighter strip, the green plane of the image is filtered by applying a morphological opening using a three-pixel diameter disc, defined in a square grid by using eight-connectivity, as structuring element.

2) *Background Homogenization*: Fundus images often contain background intensity variation due to nonuniform illumination. Consequently, background pixels may have different intensity for the same image and, although their gray-levels are usually higher than those of vessel pixels (in relation to green channel images), the intensity values of some background pixels is comparable to that of brighter vessel pixels. Since the feature vector used to represent a pixel in the classification stage is formed by gray-scale values, this effect may worsen the performance of the vessel segmentation methodology. With the purpose of removing these background lightening variations, a shade-corrected image is accomplished from a background estimate.

3) *Vessel Enhancement*: The final preprocessing step consists on generating a new vessel-enhanced image, which proves more suitable for further extraction of moment invariants-based features. Vessel enhancement is performed by estimating the complementary image of the homogenized image and subsequently applying the morphological *Top-Hat transformation* where a morphological opening operation is done by using a disc of eight pixels in radius.

B. Segmentation

Blood vessels are segmented using a described algorithm based on multiscale analysis. Two geometrical features based upon the first and the second derivative of the intensity image, maximum

gradient and principal curvature, are obtained at different scales by means of Gaussian derivative operators.[5-8] A multiple pass region growing procedure is used which progressively segments the blood vessels using the feature information together with spatial information about the eight-neighboring pixels. The lines in the line image depict the topological connectivity of the vessel structures. Let P be the set of all white pixels in a line image. Two pixels $pi, pj \in P$ are adjacent, i.e., $adj(pi, pj)$, if and only if $pj \in neigh8(pi)$, where $neigh8(p) = \{p1, p2, \dots, p8\}$ is the eight-neighborhood of p .

Definition 1 (Connected Pixels): Pixels $pi, pj \in P$ are connected, i.e., $conn(pi, pj)$, if $adj(pi, pj)$ or $\exists pc \in P - \{pi, pj\}$ s.t. $conn(pi, pc) \wedge conn(pc, pj)$.

Definition 2 (Pixel Crossing Number): Let $p1, \dots, p8$ be a clockwise sequence of the eight neighbor pixels of pixel p . Then, $xnum(p)$ is the number of black to nonblack transitions in this sequence of neighbor pixels of p .

Definition 3 (Junction): Let $white8(p) \subseteq neigh8(p)$ be the set of white pixels that are neighbors of p . The set of junction pixels in P is $YP = \{p \in P | xnum(p) > 2 \vee |white8(p)| > 3\}$. A junction is a set of connected junction pixels, i.e., $J \subseteq YP$ such that $\forall pi, pj = i \in J, conn(pi, pj)$, where $conn$ is restricted to the set YP . Then, the set of all junctions in P is JP . Fig. 4 depicts examples of junction pixels. In Fig. 4(a), they have $white8(p) = \{p2, p4, p6\}$, and $xnum(p) = 3$ due to the transitions $(p1, p2)$, $(p3, p4)$, and $(p5, p6)$. This is the straightforward case where the shaded pixel p is a junction pixel with $xnum(p) > 2$.

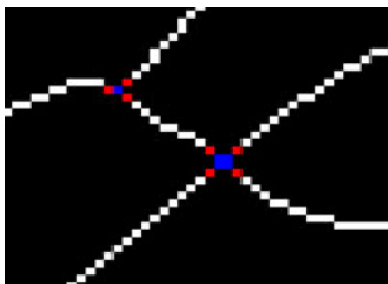


Fig. 3. Example of segment pixels (in white) with their end pixels (in red), and junction pixels (in blue).

Definition 4 (Segment): A segment s is a sequence of unique white pixels $p1, \dots, pn$ in P such that all of the following conditions are true:

- 1) $n > 0$ and $\forall i \in [1, n], pi \notin JP$
- 2) $n > 1 \Rightarrow \forall i \in [1, n - 1], adj(pi, pi+1)$
- 3) $\forall i \in \{1, n\}, |white8(pi)| = 1 \vee \exists pj \in JP$ s.t. $adj(pi, pj)$
- 4) $n > 2 \Rightarrow \forall i \in [2, n - 1], xnum(pi) = 2$.

call $p1$ and pn the *end pixels* of s . Let SP be the set of all segments in P and $NP = P - YP$ contains nonjunction pixels that are part of segments. Then, $s \in SP$ is adjacent to a junction J . Consequently, two segments $sa, sb \in SP$ are adjacent, $adj(sa, sb)$ if $\exists J \in JP$ s.t. $adj(sa, J) \wedge adj(sb, J)$. Fig 3. shows the examples of segments, endpixels and junction pixels.

IV. GRAPH TRACER

To identify vessels and represent them in the form of subsequent vessel measurements.

A. Identify Crossover Locations

Vessels in a retinal image frequently cross each other at a point or a over a shared segment

Definition 5 (Crossover Point): Given the set of white pixels P in a line image, a junction $J \in JP$ is a crossover point if and only if the number of segments that are adjacent to J is greater than or equal to 4.

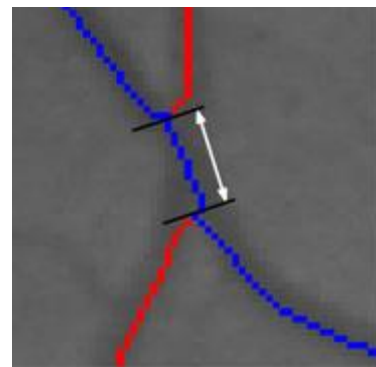


Fig.4. Example of a crossover segment.

Given the set of white pixels P of a line image, a segment $s \in SP$ is a *candidate* crossover segment if $|s| < L$ and $\exists J1, J2 \in JP$. L is a parameter to limit candidates to short segments.

Definition 6 (Directional Change Between Segments):

Given two segments sa and sb that are adjacent to a common junction, let pa and pb be the end points of sa and sb that are nearest to each other. Let va be a vector that starts on sa and ends at pa , and vb be a vector that starts from pb and ends on sb . Then, the directional change between sa and sb is given by $\Delta D(sa, sb) = \cos^{-1} \frac{va \cdot vb}{|va| |vb|}$ where $\Delta D(sa, sb) \in [0^\circ, 180^\circ]$. Intuitively, $\Delta D(sa, sb)$ measures the magnitude of a change in direction if were to go from sa to sb .

Definition 7 (Crossover Segment): Given a candidate segment seg between two junctions $J1$ and $J2$, let $Si = \{sa \in SP | adj(sa, Ji) \wedge sa = seg\}$ for $i \in \{1, 2\}$. Each Si contains two segments

sharing the same junction as one end pixel of *seg*. Let $A = \{seg\} \cup S1 \cup S2$ and $\Phi = \{\{sa, seg, sb\} / sa \in S1, sb \in S2\}$. Then *seg* is a crossover segment, i.e., *cross(seg)* is true, if all of the following conditions are true:

- 1) $\forall s, s_ \in Si, i \in \{1, 2\}, \Delta D(s, s_) > 30^\circ$
- 2) $|seg| \leq L\theta \Rightarrow$
 $[\exists sa, sb \in S1, sc, sd \in S2,$
 $3) |seg| > L\theta \Rightarrow$
 $[\forall s \in S1 \cup S2, \Delta D(seg, s) < \theta_{low}$
 $]$
 $\forall [\forall s \in S1 \cup S2, \Delta D(seg, s) <$
 θ_{high}
 $\wedge \min [sd(M(\varphi)) + sd(M(A - \varphi))]$
 $< sd(M(A))]$
 $\varphi \in \Phi$

as the segment where $\mu(s)$ is the mean intensity of the pixels in segment *s*, the bag $M(S) = \{\mu(s) / s \in S\}$ for a set of segments *S*, and *sd* is the standard deviation of the numbers in *M(S)*. Fig. 5. shows the crossover segments identified for the retinal image

C. Find the Optimal Forest

Next, in model the segments as a segment graph and use constraint optimization to search for the best set of vessel trees (forest) from the graph.

Definition 8 (Segment graph): Given the set of white pixels *P* in a line image, a segment graph $GP = (SP, EP)$, where each vertex in *SP* is a segment and an edge $ei,j = (si, sj) \in EP$ exists if $adj(si, sj)$, $si, sj \in SP, i = j$. Identified crossover segments. Typically, *GP* consists of disconnected subgraphs that are independent and can be processed in parallel.

Without loss of generality, it refer to each of these subgraphs graph *GP*. The goal is to obtain a set of binary trees from the segment graph such that each binary tree corresponds to a vessel in the retinal image.



Definition 9 (Vessel): Given a segment graph $GP = (SP, EP)$, a vessel is a binary tree, $T = (sroot, VT, ET)$ such that *sroot* is the root node, $root(T) = sroot, VT \subseteq SP$, and $ET \subseteq EP$. A set of such binary trees is called a *forest*.

A binary tree is a natural representation of an actual blood vessel as it only bifurcates. Segment end

points near the inner circle of the zone of interest are automatically identified as root pixels. The root of each tree corresponds to the root segment that contains a unique root pixel. Given a segment graph $GP = (SP, EP)$, and a set of root segments *Sroot*, let *FP* be the set of all possible forests from *GP* for each root segment in *Sroot*. The optimal forest, $F^* \in FP$ that corresponds to vessels in *GP* is given by $F^* = \text{argmin } F \in FP \text{ cost}(F)$.

V. EXPERIMENT RESULTS

The evaluate proposed method on 2446 retinal images of patients from the Singapore Malay eye study [17-18]. For each image, the line image of the retinal vessels is obtained using the miautomated retinal image analysis tool, SIVA. [12] Trained human graders then follow a protocol to verify the correctness of the vascular structure obtained, e.g., arteries, veins, crossover locations, and branch points. In use these verified vascular structures as the *gold* standard and call the corresponding vessel center lines as *clean* line images. [20]

The vessel measurements CRAE and CRVE, and average curvature tortuosity of arteries (*CTa*) and veins (*CTv*) have been found to be correlated with risk factors of cardiovascular diseases and are positive real numbers.

CRAE and CRVE are computed by iteratively mean widths of consecutive pairs of vessels in the Big6 arteries and veins [19], respectively, as follows:

$$\text{Arteries: } \hat{w} = 0.88 \cdot (w_{21} + w_{22}) / 2$$

$$\text{Veins: } \hat{w} = 0.95 \cdot (w_{21} + w_{22}) / 2$$

Where w_1, w_2 is a pair of width values and \hat{w} is the new combined width value for the next iteration. Iteration stops when one width value remains

Classifier	No of testing images	T N	TP	FP	F N	Accur (%)	Sensitivity (%)	Specificity (%)	Precision (%)
BPN	210	140	60	2	8	90	75	87	90
SVM	210	115	48	16	31	74	53	69	70

In the existing system the blood vessels are extracted using Krisch Edge Detector and the true vessels are identified using Graph Tracer. From the identified true vessels, 23 features are extracted and 15 features are selected using Fast Correlation Based Filter to speed up the classification of normal and abnormal retinal images by Back Propagation Neural Network. The performances of

the BPN classification are compared with the Support Vector Machine. During the comparison the accuracy of BPN classification is higher (90%) than the SVM's accuracy (74%).

VI. CONCLUSION

Those have presented a novel technique to identify true vessels from retinal images. The accurate identification of vessels is key to obtaining reliable vascular morphology measurements for clinical studies. The proposed method is a postprocessing step to vessel segmentation. The problem is modeled as finding the optimal vessel forest from a graph with constraints on the vessel trees. All vessel trees are taken into account when finding the optimal forest; therefore, this global approach is acutely aware of the mislinking of vessels. Experiment results on a large realworld population study show that the proposed approach leads to accurate identification of vessels and is scalable.

REFERENCES

- [1] T.Y.Wong, F. M. A. Islam,R.Klein,B. E.K.Klein,M. F.Cotch,C.Castro,A. R. Sharrett, and E. Shahar, "Retinal vascular caliber, cardiovascular risk factors, and inflammation: The multi-ethnic study of atherosclerosis (MESA)," *Invest Ophthalm. Vis. Sci.*, vol. 47, no. 6, pp. 2341–2350, 2006.
- [2] K. McGeechan, G. Liew, P. Macaskill, L. Irwig, R. Klein, B. E. K. Klein,J. J. Wang, P. Mitchell, J. R. Vingerling, P. T. V. M. Dejong, J. C. M.Witteman,M.M. B. Breteler, J. Shaw, P. Zimmet, and T. Y.Wong, "Metaanalysis:Retinal vessel caliber and risk for coronary heart disease," *Ann.Intern. Med.*, vol. 151, no. 6, pp. 404–413, 2009.
- [3] C. Y.-L. Cheung, Y. Zheng,W. Hsu, M. L. Lee, Q. P. Lau, P. Mitchell, J. J.Wang, R. Klein, and T. Y. Wong, "Retinal vascular tortuosity, blood pressure,and cardiovascular risk factors," *Ophthalmology*, vol. 118, pp. 812–818, 2011.
- [4] C. Y.-L. Cheung, W. T. Tay, P. Mitchell, J. J. Wang, W. Hsu, M. L. Lee,Q. P. Lau, A. L. Zhu, R. Klein, S. M. Saw, and T. Y. Wong, "Quantitative and qualitative retinal microvascular characteristics and blood pressure,"*J. Hypertens*, vol. 29, no. 7, pp. 1380–1391, 2011.
- [5] Y. Tolia and S. Panas, "A fuzzy vessel tracking algorithm for retinal images based on fuzzy clustering," *IEEE Trans. Med. Imag.*, vol. 17,no. 2, pp. 263–273, Apr. 1998.
- [6] H. Li, W. Hsu, M. L. Lee, and T. Y. Wong, "Automatic grading of retinal vessel caliber," *IEEE Trans. Biomed. Eng.*, vol. 52, no. 7, pp. 1352–1355,Jul. 2005.
- [7] E. Grisan, A. Pesce, A. Giani, M. Foracchia, and A. Ruggeri, "A new tracking system for the robust extraction of retinal vessel structure," in *Proc. IEEE Eng. Med. Biol. Soc.*, Sep. 2004, vol. 1, pp. 1620–1623.
- [8] Y.Yin,M.Adel, M. Guillaume, and S. Bourennane, "Aprobabilistic based method for tracking vessels in retinal images," in *Proc. IEEE Int. Conf.Image Process.*, Sep. 2010, pp. 4081–4084.
- [9] M. Martinez-Perez, A. Highes, A. Stanton, S. Thorn, N. Chapman, A.Bharath, and K. Parker, "Retinal vascular tree morphology: A semiautomatic quantification," *IEEE Trans. Biomed. Eng.*, vol. 49, no. 8,pp. 912–917, Aug. 2002.
- [10] H. Azegrouz and E. Trucco, "Max-min central vein detection in retinal fundus images," in *Proc. IEEE Int. Conf. Image Process.*, Oct. 2006,pp. 1925–1928.
- [11] V. S. Joshi, M. K. Garvin, J. M. Reinhardt, and M. D. Abramoff, "Automated method for the identification and analysis of vascular tree structures in retinal vessel network," in*Proc. SPIEConf.Med. Imag.*, 2011, vol. 7963,no. 1, pp. 1–11.
- [12] B. Al-Diri, A. Hunter,D. Steel, andM.Habib, "Automated analysis of retinal vascular network connectivity," *Comput. Med. Imag. Graph.*, vol. 34,no. 6, pp. 462–470, 2010.
- [13] K. Rothaus, X. Jiang, and P. Rhiem, X. Jiang, and P. Rhiem, "Separation of the retinal vascular graph in arteries and veins based upon structural knowledge," *Imag. Vis. Comput.*, vol. 27, pp. 864–875, 2009.
- [14] R. L. Graham and P. Hell, "On the history of the minimum spanning tree problem," *IEEE Ann. Hist. Comput.*, vol. 7, no. 1, pp. 43–57, Jan.-Mar.1985.
- [15] C. All'ene, J.-Y. Audibert, M. Couprie, and R. Keriven, "Some links between extremum spanning forests, watersheds and min-cuts," *Imag. Vis.Comput.*, vol. 28, pp. 1460–1471, 2010.
- [16] J. Cousty, G. Bertrand, L. Najman, and M. Couprie, "Watershed cuts:Minimum spanning forests and the drop of water principle," *IEEE*

Trans. Pattern Anal. Mach. Intell., vol. 31, no. 8, pp. 1362–1374, Aug. 2009.

[17] A. W. P. Foong, S.-M. Saw, J.-L. Loo, S. Shen, S.-C. Loon, M. Rosman, T. Aung, D. T. H. Tan, E. S. Tai, and T. Y. Wong, “Rationale and methodology for a population-based study of eye diseases in Malay people: SiMES,” *Ophthalm. Epidemiol.*, vol. 14, no. 1, pp. 25–35, 2007.

[18] S. Garg, J. Swamy, and S. Chandra, “Unsupervised curvature-based retinal vessel

segmentation,” in *Proc. IEEE Int. Symp. Biomed. Imaging*, Apr. 2007, pp. 344–347.

[19] C. Y.-L. Cheung, W. Hsu, M. L. Lee, J. J. Wang, P. Mitchell, Q. P. Lau, H. Hamzah, M. Ho, and T. Y. Wong, “A new method to measure peripheral retinal vascular caliber over an extended area,” *Microcirculation*, vol. 17, pp. 1–9, 2010.

[20] W. E. Hart, M. Goldbaum, P. Kube, and M. R. Nelson, “Automated measurement of retinal vascular tortuosity,” in *Proc. AMIA Fall Conf.*, 1997, pp. 459–463.